
Article:
Povey, MJW orcid.org/0000-0002-9740-2596 (2016) Nucleation in food colloids. Journal of Chemical Physics, 145 (21). 211906. ISSN 0021-9606

https://doi.org/10.1063/1.4959189

Nucleation in food colloids

Malcolm J. W. Povey, School of Food Science and Nutrition, The University of Leeds

For The Journal of Chemical Physics, Special Topic Issue on **Nucleation: New Concepts and Discoveries.**

Abstract

Nucleation in food colloids has been studied in detail using Ultrasound Spectroscopy. Our data shows that classical nucleation theory (CNT) remains a sound basis from which to understand nucleation in food colloids and analogous model systems using n-alkanes. Various interpretations and modifications of CNT are discussed with regard to their relevance to food colloids. Much of the evidence presented is based on ultrasound velocity spectrometry measurements which has many advantages for the study of nucleating systems compared to light scattering and NMR due to its sensitivity at low solid contents and its ability to measure true solid contents in the nucleation and early crystal growth stages. Ultrasound attenuation spectroscopy also responds to critical fluctuations in the induction region. We show however, that a periodic pressure fluctuation such as a quasi-continuous (as opposed to a pulse comprising only a few pressure cycles) ultrasound field can alter the nucleation process, even at very low acoustic intensity. Thus care must be taken when using ultrasound techniques that the measurements do not alter the studied processes. Quasi-continuous ultrasound fields may enhance or suppress nucleation and the criteria to determine such effects are derived. The conclusions of this paper are relevant to colloidal systems in foods, pharmaceuticals, agro-chemicals, cosmetics and personal products.

1. Introduction

1.1. What are Food Colloids

Whilst food colloids are ubiquitous and will be found in any domestic refrigerator and food cupboard, not all food colloids contain crystalline material. Examples of food colloids in which crystal nucleation plays a critical role during processing are fatty spreads including butter and margarine, ice cream[1], clotted and whipped cream[2], milk fats in general and sugar-fat confectionery creams. These are all examples where a gel (or soft solid) is created through the crystallisation of a colloidal dispersion, thereby creating structure from an otherwise liquid system[3]. Many of these emulsions are precursors for very many more foods such as breads, cakes, meringues and mousse. Emulsion crystallisation of oils is also used to encapsulate valuable nutrients which would otherwise be

unstable during storage but are required to release the bio-active component when digested (for a recent review see [4]). Similar systems exist in creams manufactured in the pharmaceutical, agro-chemical, cosmetics and personal products industries.

The dispersed phase diameter may vary in food colloids from a few nanometres in size (micelle, swollen micelle) and comprising a few tens of molecules through to a few micrometres, the upper limit generally controlled by the point at which the buoyancy of the dispersed phase overcomes the thermally induced Brownian motion which keeps the particles dispersed. In many food colloids, Brownian diffusion may be greatly reduced through a variety of particle interactions which give rise to weakly connected (attractive interaction energies of a few k_BT) systems of particles. Paradoxically, whilst reducing the thermal motion which overcomes gravitational destabilisation, these interactions may transform the colloidal substance into a weakly gelled system which prevent or suppress gravitational destabilisation and permit larger sized particles to be stable than would otherwise be the case.

1.2. Crystallisation in Food Colloids

Crystal nucleation kinetics are transformed once a bulk liquid melt is dispersed as small droplets to form a colloidal substance comprising a liquid suspending phase and the dispersion of particles which are initially liquid then transform into solid. In many food colloids, the transformation to crystalline solid of the dispersed liquid phase is only partial, giving rise to a dispersion of solid inside a dispersed liquid phase. Cow's milk is an example of such a colloidal system, where the oil droplets dispersed in the aqueous suspending phase themselves contain crystalline fat particles. Complicating matters is the fact that the amount of crystalline material depends on the time of year and the animal feeding regime. The nucleation of fat particles in the oil droplets which form the milk dispersion is one of the first stages in butter manufacture. The fat grows out of the oil droplets and when the needle like crystals from nearby droplets collide they sinter to form a space filling network which proffers the solid properties of the butter soft solid. This network traps water droplets within it, locking them away from microbial and mould growth, creating a product with a shelf life of months. When the butter enters the mouth, the crystal network melts, the system inverts to an oil-in-water emulsion and rather than an oily mouthfeel a pleasant watery feel forms part of the eating experience.

The study of the crystallisation of food emulsions over many years in the School of Food Science and Nutrition in Leeds and the ready availability in our laboratory of colloid manufacture and characterisation provided the wherewithal for our studies of crystal nucleation kinetics in model and real

food colloids. The combination of this resource together with a unique combination of ultrasound and acoustic techniques has enabled the new concepts and discoveries described herein.

1.3. The Study of Nucleation in Food Colloids

Emulsion crystallisation has many advantages for the study of crystal nucleation because it permits the reduction of the crystallising volume to that of a single small droplet whose size (hence volume and surface area) can be controlled. It therefore makes it possible to study the effects of volume and surface – measurement of isothermal crystallisation rates in an emulsion can even give the Gibbs Free Energy for nucleation[5]. It is also possible to identify and isolate the seed crystals of various sorts (sometimes called catalytic impurities) which almost invariably act as the nuclei in food colloids [6] – homogeneous nucleation is very unusual and I am not aware of any industrial processing operation which currently relies on homogeneous nucleation. However, it has been shown that through the use of surfactants, the surface energy of a very small oil droplet can be reduced to the point where surface homogeneous nucleation of the droplet becomes more or less certain.[5]. Processing operations generally involve seeding the melt and introducing shear.

As mentioned above, another advantage of emulsion crystallisation for fundamental studies of crystal nucleation is that a great deal of control over the surface can be achieved through the use of a wide variety of surfactants which lower surface energy and may also act as surface heterogeneous nuclei [7-12]. It is also worth noting that at constant dispersed phase volume, as the size reduces the surface area increases and that this interfacial region is far from simple, contributing to surface heterogeneous nucleation effects in a number of ways, some of which could be regarded as unexpected. For example, in 100 nm droplets of trilaurin, 7% of the volume is directly influenced by the surface which generally comprises a solution of surfactant and oil, causing surface melting point depression and lowered surface energy.

1.4. The Production of Food Colloids

Food Colloids are produced in a number of ways. The most common is high pressure homogenisation using water or oil-soluble surfactants to reduce the interfacial energy and stabilise the dispersed phase [13–15]. Power ultrasound may also be used and can produce fine stable emulsions [16,17], however for water containing systems the associated cavitation may produce undesirable oxidative rancidity and other unpleasant off-flavours, such as a metallic taste associated with erosion of the sonotrodes used to apply the ultrasound to the processed material. Another technique is the ultrasound whistle, also called the Pholmann whistle or jet edge transducer [18] in which a blade vibrates at ultrasound frequency as a result

of fluid passing across it and the blade motion breaks up the particulate phase. In some cases micro-emulsions may be produced, a good example being the Ouzo effect where anise oil dissolved in ethanol is precipitated out of the ethanol through the addition of water which acts as an 'anti-solvent', causing the spontaneous nucleation of droplets small enough to scatter light (80 nm to 500 nm) imparting a milky appearance to the drink and forming a colloidal dispersion of oil droplets suspended in an ethanol/water drink [19]. Micro-emulsions differ from most Food Colloids in that they do not require the use of surfactants and have a near zero surface energy, requiring only a very simple fluid addition step. However, most micro-emulsions have a narrow range of stability and whilst occupying an important niche have limited application in foods.

1.5. Power Ultrasound and Sonocrystallisation

There is considerable literature and interest in the use of high power ultrasound for the control of crystal nucleation [20–25]. Power ultrasound interacts with crystal nucleation and growth in a number of ways and in general is not well understood. This author has shown that stable cavitation [26] can induce the crystallisation of ice simply through bubble wall motion [27–29]. Transient cavitation can induce crystallisation and can also melt the crystals so produced, depending on the power levels. Pressure and heating effects may also occur in the absence of cavitation, together with the concentration of crystals at pressure anti-nodes [30], thereby modifying secondary nucleation and crystal morphology. On the whole, power ultrasound and sono-crystallisation is a complex and poorly understood area in which successful applications have been developed as much by empiricism as anything else. However, conventional sonocrystallisation using power ultrasound suffers from the same disadvantages as the use of power ultrasound for emulsification of many food colloids – off flavours, oxidative rancidity and irreproducibility.

1.6. Ultrasound as a Diagnostic Tool in Crystallisation

This author has developed pulse-echo time-of-flight (PE) techniques for the measurement of crystallinity [5,6,31–35], for example solid fat content (SFC) in systems such as fatty spreads and mayonnaise [36]. These methods can also be used to determine water content [37]. More recently PE has been used to monitor protein crystallisation [38]. The PE technique used for studying isothermal crystal nucleation described below is described in detail in [37].

Shear reflectance techniques have most recently been used to study the isothermal nucleation of cocoa butter [39,40].

2. Classical Nucleation Theory in Food Colloids

Crystal formation can be considered in three stages: (i) the clustering of molecules into a prenucleation embryonic (unstable) state of indeterminate structure, either randomly within a volume (homogeneous nucleation) or in two dimensions on a pre-existing surface provided by a seed crystal or catalytic impurity (heterogeneous nucleation), (ii) the formation of crystal nuclei with a definite structure (usually the final polymorph) and the potential to create a site for crystal growth and then (iii) the growth of the crystal from the so formed nucleus. The metastable zone exists between the saturation limit and the viable nucleation limit. It is also necessary to distinguish between crystallisation from a melt and crystallisation from a solution. This may be a problem because in many foods, distinguishing between crystallisation from a melt and from a solution can be difficult and in these cases accurate determination of the phase diagram may be very difficult – high melting point forms may be soluble in lower melting, still liquid forms even if they are well below their melting point and hence expected to crystallise out. For example, in the case of what is generally regarded as a 'pure' fat – Cocoa butter – a great deal of variation is found in its melting curve, according to origin (Figure 1).

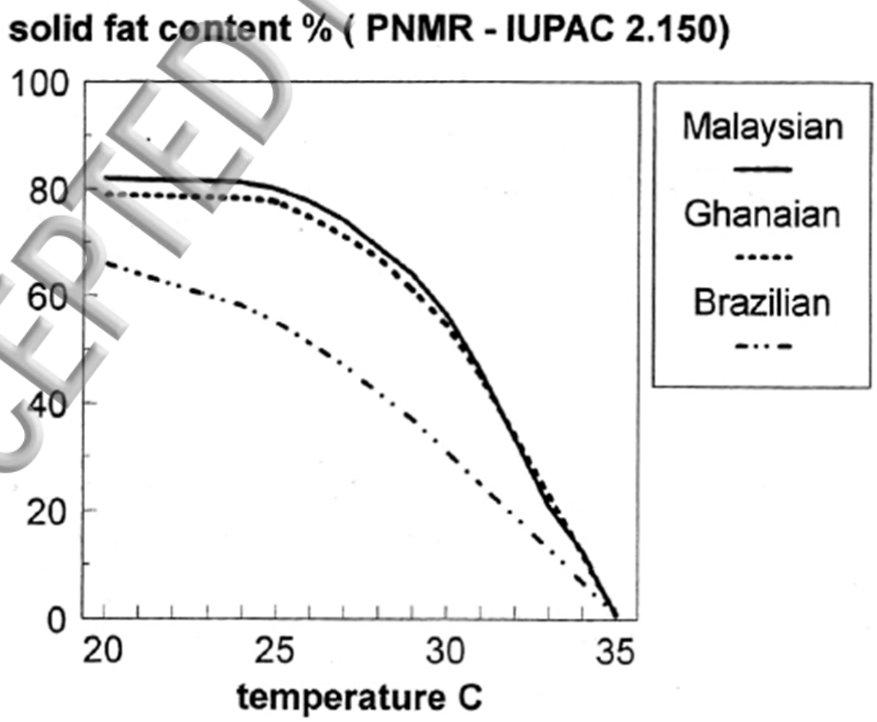

Figure 1 Solid fat content (SFC) of cocoa butters from different growing areas obtained by NMR measurements [41]

For a more complex fat such as anhydrous milk fat (AMF) part of the fat remains liquid at ambient temperatures and different components of the fat crystallise selectively from 'solution'. It is quite possible to zone refine and thereby purify fat mixtures this way.

The reader is referred to various reviews for an overview of crystal nucleation in bulk fluids and the additional properties which dispersion as a colloid imparts on the behaviour of the fluid phase of the crystalline material [42–45 5 46 47 48 49]. There follows a summary of the important features.

2.1. Bulk saturated material

With regard to the bulk saturated material, there is a metastable phase between the saturation limit and the viable nucleation limit. This is described in detail in a recent paper by Threlfall and Coles[50].

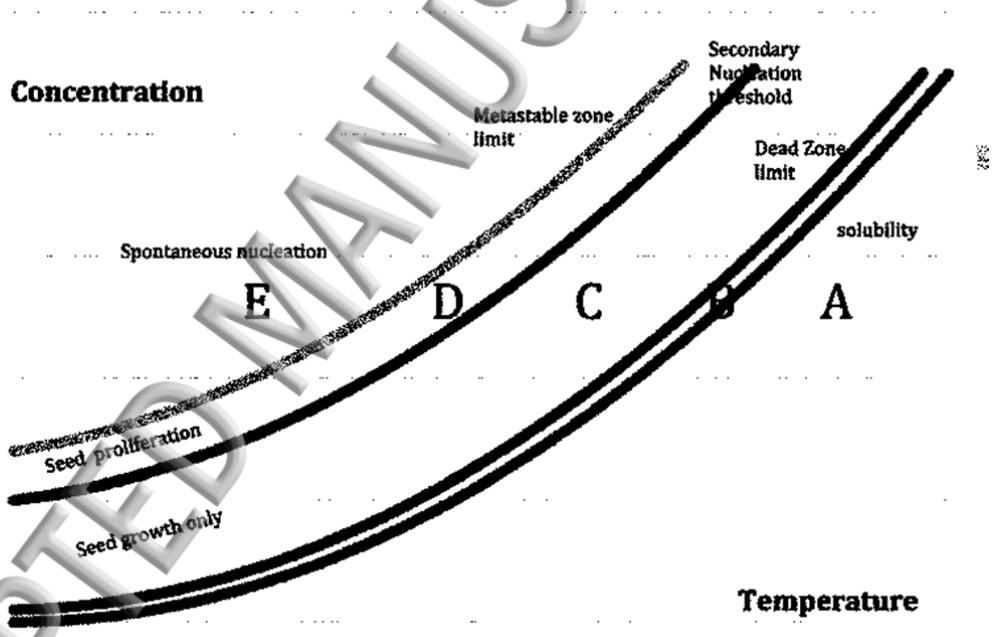

Figure 2 The generalised solution crystallisation diagram, showing the thermodynamic solubility curve, the dead zone limit, the secondary nucleation threshold and the metastable limit, reproduced with permission from CrystEngComm 18, 369 (2016). Copyright 2016 Royal Society of Chemistry [50].

Referring to Figure 2, the line of saturation (delineating the transition from solubility to saturation, A-B) can be determined through measurements of the temperature dependence of the velocity of sound which has a different slope in the two regions. In B, viable nuclei don't form although the system is saturated and a degree of super saturation is necessary before nucleation can occur, instead molecules cluster into a prenucleation embryonic (unstable) state of indeterminate structure,

appearing in a transient form and then disappearing, creating so-called critical density fluctuations [51], [52–54]. In C stable nuclei appear, which whilst stable are too small to scatter light and whose numbers are too small to significantly affect the crystal solid content. Nevertheless, in region C, the nuclei have a definite structure (not always the final polymorph) and the potential to create a site for crystal growth. It is only when the secondary nucleation threshold is crossed and we enter D, that proliferation of seeds occurs and detectable growth of solid crystalline material occurs (It is in this region that SAXS/WAXS will evidence crystal structure). Finally, the metastable zone limit is reached and crystal growth proceeds, secondary nucleation and spontaneous nucleation occur. It needs to be born in mind that the transitions C-D and D-E are time and volume dependent and the lines C-D and D-E will move to lower concentration and higher temperature at longer times.

Considering only the crystal nucleation (as described above) and crystal growth stages; in the nucleation stage submicroscopic viable crystal nuclei are formed which develop into larger crystals during the subsequent growth stage. With homogenous nucleation the crystals are formed directly from the liquid. Heterogeneous nucleation is nucleation mediated by foreign particles already present in the liquid. Secondary nucleation is nucleation mediated by pre-existing crystals.

The temperature, concentration and pressure at which these events occur and the speed (the temporal history of all the independent and dependent variables) at which they take place have an important impact on the performance and properties of the final crystalline material.

2.2. Ultrasound studies of nucleation in supersaturated solution

How does this generalised view of Threlfall and Coles map onto our observations using ultrasound velocity measurements? In Figure 3 region I, which corresponds to A in Figure 2, the solution was quickly cooled down from 40 °C to 28 °C to prepare the supersaturated solution. There were no crystals in the solution, and this was verified by comparing the velocity value to the temperature dependent pure solution velocity data.

After region I in Figure 3, the solution temperature was kept constant at 28 °C, region II corresponding to the induction period, note that the velocity increases slightly in this region indicating a reduced adiabatic compressibility, probably associated with changes in ordering in the liquid followed later by the formation of a few seed crystals (C in Figure 2). Since the solid content determined by ultrasound is a function of the properties of both the suspending fluid and the emerging solid phase, it is not possible to distinguish between compressibility changes occurring due to liquid ordering and solid ordering and the amount of seed crystals cannot be quantified in this region, except to say that it is <<0.5% by

volume. In region III (corresponding to C and D in Figure 2) the velocity decreased as the amount of the crystals increased. After all the crystals came out from the solution, the sound velocity remained constant. The sound velocity change in Region III, calibrated against the measured sound velocity for a given concentration was used to calculate the crystal compressibility depending on the modified Urick model and then the crystal solids content (Figure 4).

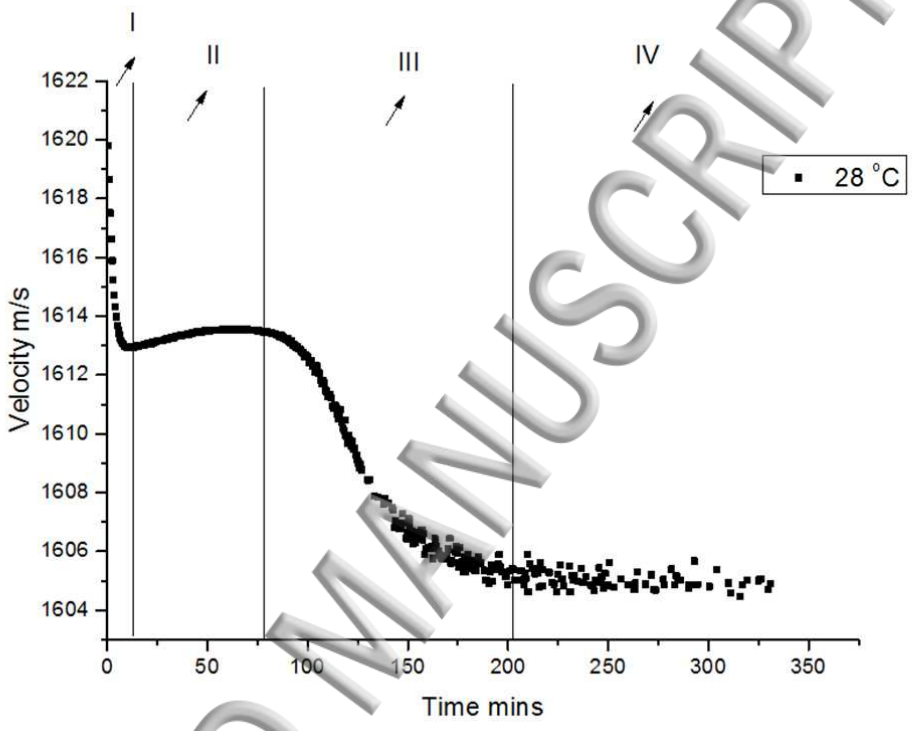

Figure 3 Sound velocity measurement of stirred 45 w% copper sulphate solution at a fixed temperature of 28 °C

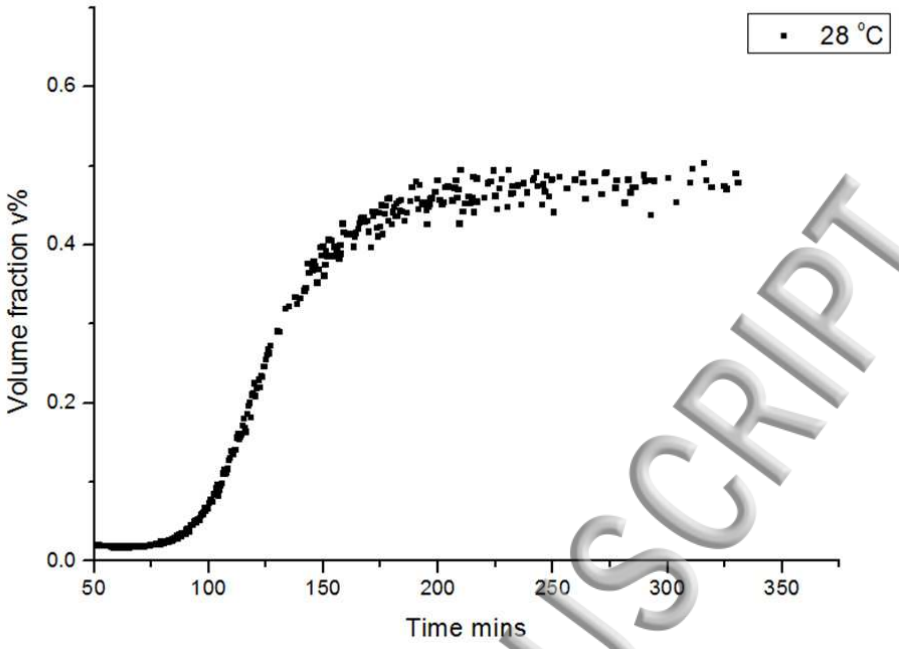

Figure 4 Crystal volume fraction evolution during the crystallization process for 45 w% copper sulphate solution fixed at a temperature at 28 °C [55]

2.3. A brief comparison between ultrasound, DSC, Infra-red and NMR

An important observation when comparing DSC measurements with ultrasound measurements is that the ultrasound measurements directly respond to the density and adiabatic compressibility changes associated with crystallisation processes, even under isothermal conditions whereas DSC cannot operate isothermally unless there are large enthalpy changes occurring. For many industrial processes, DSC temperature scanning rates are unrealistically fast and therefore it is difficult with DSC to investigate the temporal dimension of phase diagrams except at very short times. In fact, ultrasound data on crystallisation processes is better under isothermal conditions because otherwise the impact on the speed of sound of temperature changes has to be accounted for (See for example region 1 in Figure 3). So DSC and ultrasound should be regarded as complementary techniques.

Light scattering techniques are widely used to study crystallisation processes[56–62]. Ultrasound has advantages in comparison for optically opaque and/or highly absorbent materials and also responds to changes in particles whose size is below that where light scattering is insignificant, typically this limit is around 80 nm, hence its capabilities for the study of nucleation.

pNMR is a standard method for the measurement of solid fat content[63] and whilst water reduces accuracy methods have been developed for the measurement of solid fat content in food emulsions[64–66]. In comparison, ultrasound is more sensitive and accurate at low solid contents, however it becomes increasingly inaccurate at later stages in crystal growth where crystal networks are developing. An initially very promising development in NMR is Fast Field Cycling NMR (FFCNMR) [67,68]. Recent studies in our laboratory suggest that the mobility of fat molecules can be compared using FFCNMR, providing a new insight into the process of transition from liquid to solid in nucleation processes.

2.4. Bulk material dispersed as a colloid

In essence, the same procedure is used as described for the bulk material to determine the solids content of a dispersed phase of an emulsion, with corrections made for droplet size ultrasound scattering and volume fraction. The rate of increase of solids gives the isothermal crystallization rate. The first experiments on the determination of crystal nucleation kinetics using Classical Nucleation Theory (CNT) concepts and using emulsion crystallization as an experimental technique was by Turnbull & Cormia (1961)[43] whose approach we have followed in most respects.

2.5. Some comments on CNT

The proposition of CNT last century by Fisher et al. 1948 [42] is essentially an energy one which may be applied to any nucleation process, not only crystal nucleation. This approach is often counter posed to the stepwise molecular self-assembly approach such as that discussed by Davey et al, 2013[46]. However, the essence of CNT (for a review see [47]) is the energy balance between surface energy terms and bulk solid energy in the formation of an energy threshold[69]. Critiques of CNT centre (a) on the difficulties of calculating the surface energy and (b) the indisputable fact that a series of steps may form part of the pathway to the formation of a stable nucleus. Neither (a) nor (b) can detract from the fact that the surface to volume energy balance is a crucial and often calculable factor in nucleation kinetics.

3. Surface and volume heterogeneous nucleation

In [5] the surface and volume energy terms in units of $k_B T$ is calculated for a droplet of trilaurin in the presence of a surface energy lowering surfactant (Figure 5). For trilaurin in water stabilised by a surfactant lowering the surface tension to 1 mN m^{-1} the critical nucleus size is 4 nm.

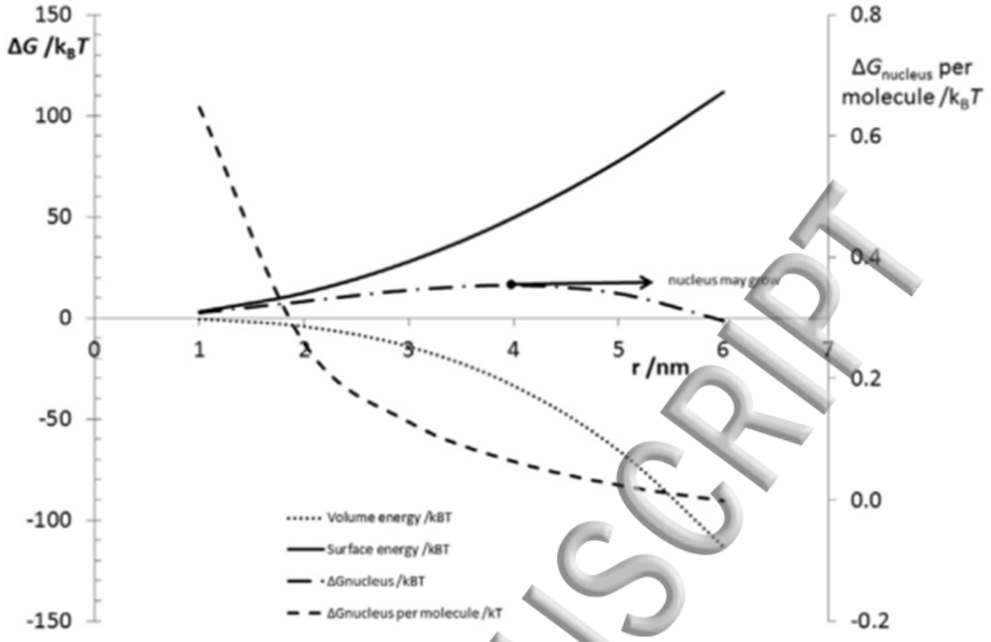

Figure 5 Plot of surface and volume energy in units of KBT as a function of particle radius for a trilaurin droplet, together with the estimated attachment energy per molecule in units of k_BT. The surface tension in this plot is 1 mN/m and the enthalpy change of the trilaurin in the alpha form is taken as 167 J/kg. [5]

In that paper it is also shown that in colloidal systems it is possible to reduce the probability of finding a critical nucleus in any one droplet to well below one and yet obtain an increasing probability of nucleation arising from inter-droplet collision mediated nucleation. As a result, undercooling initially falls as droplet size is decreased at a constant dispersed phase volume fraction and then rises again as the Brownian motion mediated collision processes take over.

Through the emulsion crystallisation method, it is possible to control droplet size, dispersed phase volume and surface energy thereby giving control over nucleation which is unavailable in bulk fluids and permitting measurement of surface Gibbs energy for nucleation, determination of the nature of nucleation (surface or volume, homogeneous or heterogeneous), partial coalescence and energy barrier to coalescence. Together with ultrasound spectroscopy, a unique facility exists for the characterisation of crystal nucleation in food colloids.

4. The theory of coupled pressure and heat fluctuations

4.1. Introduction

In [45] it is shown that a continuous sinusoidal ultrasound pressure wave of 2 MHz frequency and a power level of 3 watts can suppress the nucleation of eicosane. In these experiments the undercooled fluid was maintained

at constant temperature, removing the small amount of heat transferred to the entire undercooled fluid by the insonifying field. We show here that such low power levels may nevertheless pump sufficient energy into a crystal embryo to suppress its transformation into a stable nucleus. It is suggested here that such energy transfer occurs only between the suspending fluid and the embryo and since embryo's comprise a very small part of the system mass only very small amounts of energy need be involved, the important relation being between the volume energy (latent plus free energy) and the surface energy of the embryo. This energy transfer occurs because of the different thermal properties and acoustic properties of the suspending fluid and the embryo which in the presence of a continuous oscillating pressure field (ultrasound) causes a difference in the oscillating temperature generated in the suspending and dispersed phase. All other things being equal and *ignoring classical attenuation*, there would be no net energy flow because the resultant heat flow on the compression phase would be equal and opposite to that on the expansion phase. However, when the area over which the heat flow occurs is taken into account, there is a small difference between the area through which heat flows which is slightly greater on the expansion phase than on the compression phase (Figure 6). This leads to a 'rectification' in the heat transfer with a small amount of heat transferred into the embryo on each cycle. Energy is therefore pumped into the embryo over many cycles, thus we would not expect to see this effect in pulsed ultrasound.

The difference in attenuation coefficient between the suspending and dispersed phases will also produce a differential heating effect whose magnitude is estimated in section .

4.2. Heat flow between a nucleus and its suspending medium

In [37] the theory of acoustic scattering in colloidal systems is developed in detail and that theory contains a solution for thermal diffusion around an oscillating colloidal particle. In [5] it is suggested that thermal diffusion must play an important role in crystal nucleation in colloidal systems and a simple derivation is given here for the case of low amplitude pressure oscillations in an emulsion.

We calculate here the heat flow between a small nucleating particle (crystal embryo) suspended in a fluid and the suspending phase as a result of a continuous low power oscillating acoustic field. We assume that the entire system is maintained at constant temperature and consider only the temperature difference between the suspending phase and the crystal embryo.

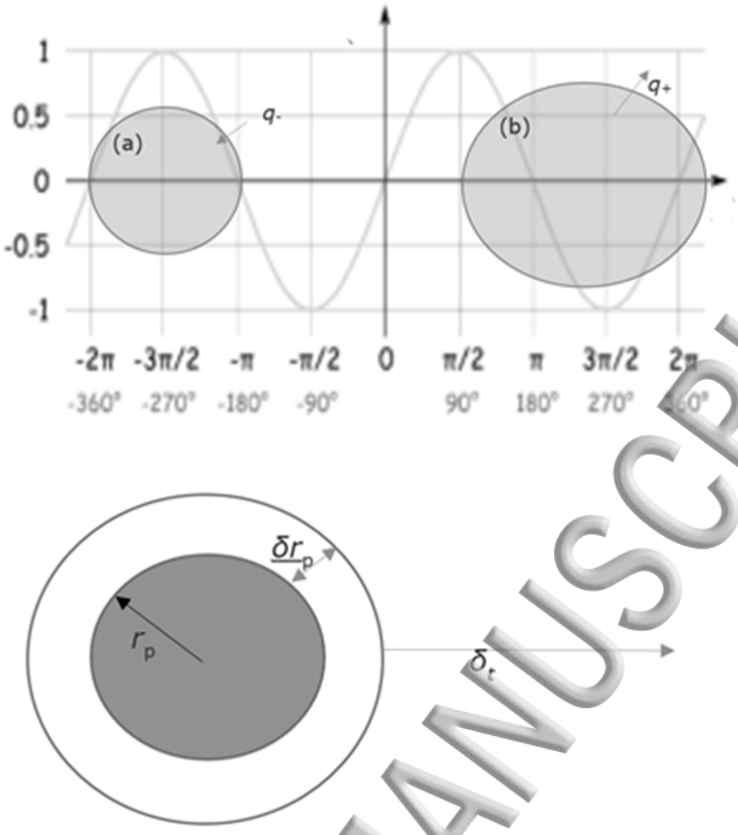

Figure 6 diagram and cartoon of droplet oscillating in a sinusoidal pressure field. r_p is drop radius, δ_t is the thermal diffusion length at the pressure field frequency f, δr_p is the change in drop radius due to the oscillating pressure field. Heat flow is proportional to area and the temperature gradient reverses when the pressure switches from positive to negative. On the positive pressure cycle (a) the droplet has a smaller surface area than on the negative pressure cycle (b). The temperature gradient reverses when the phase is zero so the heat flow is rectified because on the positive pressure half cycle (a) the droplet has a smaller surface area than on the negative pressure half cycle (b). The temperature gradient reverses when the phase is zero and the heat flow is rectified because it is proportional to the surface area of the droplet which is smaller on the positive pressure cycle than it is on the negative pressure half cycle, so that $q_+ \neq q_-$.

The temperature θ of a medium fluctuates with pressure [70] according to

Equation 1

$$\Delta\theta = \frac{\Delta p}{\beta}\left(\kappa - \frac{1}{\rho c^2}\right)$$

Where the instantaneous pressure fluctuation Δp is given by

Equation 2

$$\Delta p = \Delta p_0 sin\omega t$$

The volume coefficient of thermal expansivity β is

Equation 3

$$\boldsymbol{\beta = \frac{1}{V}\frac{\partial V}{\partial \theta}}$$

And the amplitude of the pressure fluctuation Δp_0 is related to the acoustic intensity I (W m^{-2}) through

Equation 4

$$\boldsymbol{I = {(\Delta p_0)^2}/{\rho c}}$$

Here V is volume (m^3); Δp is instantaneous pressure (Pa) and the adiabatic compressibility κ (Pa^{-1}) is related to the velocity of sound c in a fluid medium through $c = \frac{1}{\sqrt{\kappa\rho}}$ (m s^{-1}). β is the volume coefficient of thermal expansivity (K^{-1}); ρ is density (kg m^{-3}); $\omega = \frac{2\pi}{f}$ is the radial frequency of the pressure wave (rad s^{-1}) and f is frequency (Hz). We will also use the following definitions: k (m^{-1}) is the pressure wave vector $\left(\frac{2\pi}{\lambda}\right)$; λ is wavelength (m).

An equivalent equation to Equation 1 applies to the droplet phase

Equation 5

$$\Delta\theta' \cong \frac{\Delta P}{\beta'}\left(\kappa' - \frac{1}{\rho' c'^2}\right)$$

Where all the quantities are as defined above and primed quantities apply to the dispersed or droplet phase. Equation 5 is only approximately true because (a) Equation 1 is true for an infinite medium and (b)

Heat will flow into and out from the drop, driven by the difference in temperature between the suspending phase and the droplet.

Equation 6

$$\Delta(\Delta\theta) = \Delta\theta' - \Delta\theta$$

Using the data in Table 1for a hexadecane oil-in-water emulsion this quantity is 1 μK in a 1 MHz oscillating pressure field with an amplitude of 4 kPa, equivalent to a field intensity of 10 W m^{-2}.

Noting all the time that the temperature fluctuation $\Delta\theta$ is an oscillating one, approximately adiabatic and is not isothermal. In each pure phase, this heat flow between the pressure wave and the medium is adiabatic because the temperature rise on one half cycle is balanced by the equivalent temperature fall on the second half cycle. However, once an interface is established, such as that between the droplet and its suspending medium, the situation becomes more complicated. The temperature difference between the two phases will drive heat flow

between them, although this is still not necessarily thermally dissipative heat flow. However, because the temperature gradient reverses between the two half cycles of the pressure wave and heat flow across the boundary is proportional to area, the possibility of rectification of that heat flow arises because the surface area of the drop is greater during the expansion phase than during the compression phase. Determination of the direction of heat flow depends on a detailed calculation of Equation 6 and of the dynamic surface area which is calculated below.

Equation 7

$$\kappa = -\frac{1}{V}\frac{\delta V}{\delta p}$$

In order to obtain the dynamic surface area we need to integrate Equation 7 which gives

Equation 8

$$V(t) = V_p exp(\Delta p_0 sin\omega t)$$

Where $V(t)$ is the time dependent volume of a droplet whose mean volume is V_p and Δp_o is maximum pressure displacement of the insonifying, oscillating pressure field as given by Equation 2.

The instantaneous surface area is then

Equation 9

$$A(t) = 4\pi r_p^2 = 4\pi\left\{\frac{3V_p exp\left(\kappa\Delta p_0 sin(\omega t)\right)}{4\pi}\right\}^{2/3}$$

The instantaneous heat flow $q(t)$ (J s^{-1}) into the droplet of volume V_p is obtained approximately by assuming that all heat flows take place over the thermal diffusion length δ_t in the suspending phase so that

Equation 10

$$q(t) = \frac{\tau A(t)\Delta(\Delta\theta)}{\delta_t}$$

Where τ is the thermal conductivity of the suspending phase (W m^{-1} K^{-1}).

Bear in mind that the temperature distribution is established by Equation 6 and not by the unsteady state heat transfer equation.

Using the data below for hexadecane oil-in-water emulsion it can be shown using the above equations that heat will be differentially transferred from the insonifying pressure field into the droplets, initially without significant heating of the surrounding fluid.

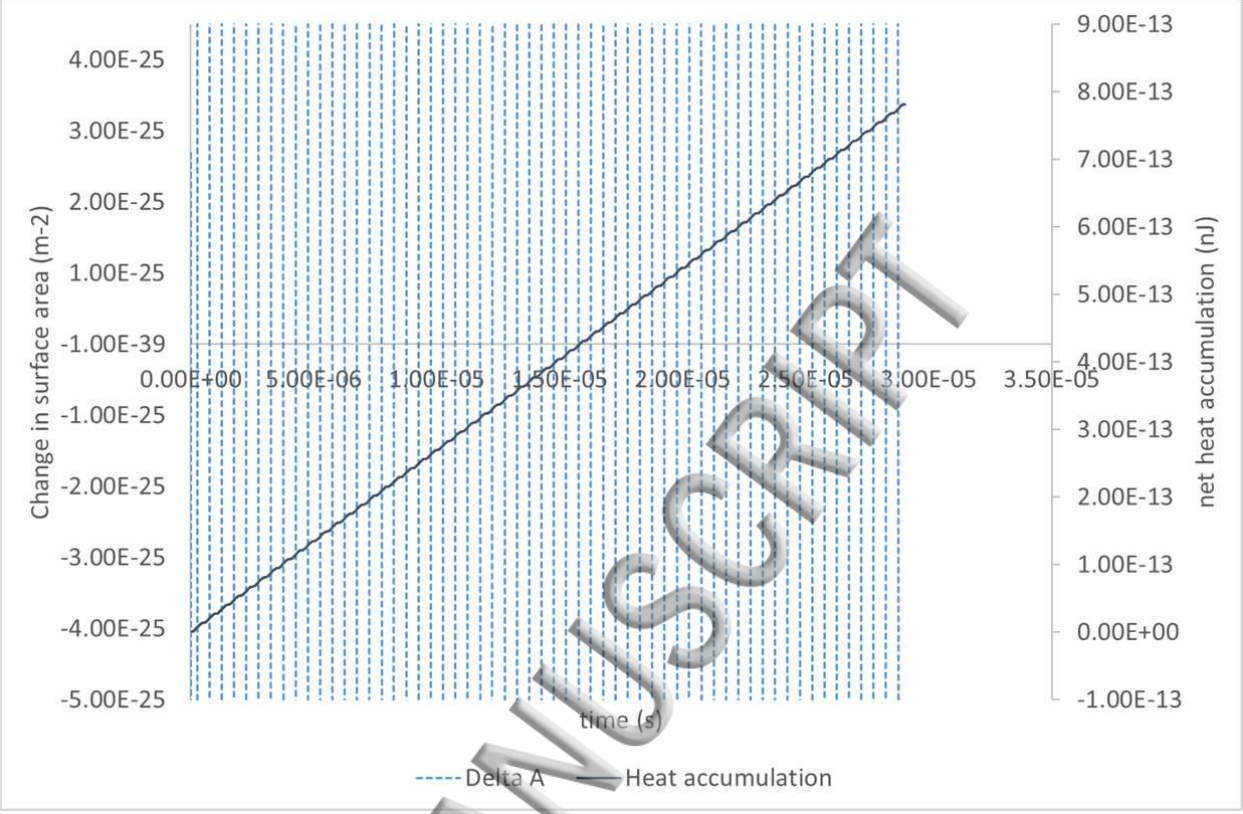

Figure 7 Numerical calculation of rectified heat flow for a 4-nm hexadecane drop at 25 C (the critical nucleus size in Figure %) an insonifying frequency of 1 MHz and an acoustic intensity of 10 W m^{-2} for the first few cycles of the insonifying field. Delta A is the change in surface area arising in response to the changing pressure field. Heat accumulation in the droplet is calculated using Equation 10. Data is from Table 1..

Symbol	Property	Value	Units	Status			
I_0	sound intensity	10	w m^{-2}	given			
ω	radial frequency	6283185.3		calculated			
f	sound frequency	1.00E+06	Hz	given			
p_0	Maximum pressure deviation	3.86E+03	Pa	calculated			
T	Period of wave	1.00E-06	s	calculated			
$r_{particle}$	Particle radius	4.00E-9	m	given			
$V_{particle}$	Particle volume	2.68E-25	m^3	calculated			
			Suspending phase properties *Water at 25 °C*			Dispersed phase properties n-hexadecane at 25 °C	
ΔH_f	Latent heat of fusion					167	J kg^{-1}
	Latent heat of fusion for the particle					3.45E-20	J
λ	wave length v/f	0.001497	m	calculated			
α	attenuation	0.00216	Np m^{-1} MHz^{-2}			0.009725	Np m^{-1} MHz^{-2}
β	volume expansivity (thermal dilatability)	0.000257	K^{-1}	given	β'	0.00091	K^{-1}
k	wave vector ω/v	4197.1846	m^{-1}	calculated	k'	4687.2	m^{-1}
γ	ratio of specific heats	1.05		given	γ'	1.05	
τ	thermal conductivity	0.59525	W m^{-1} K^{-1}	given	τ'	0.14	W m^{-1} K^{-1}
C_p	Heat capacity at constant pressure	4178.476	J kg^{-1} K^{-1}	given	Cp'	2217	J kg^{-1} K^{-1}
σ	thermal diffusivity k/ρCp	1.431E-07	W m^{-1} K^{-1}	calculated	σ'	0.00275	W m^{-1} K^{-1}
v	velocity of sound	1497	m s^{-1}	given	v'	1340.5	m s^{-1}
ρ	density	995.24	kg m^{-3}	given	ρ'	770	kg m^{-3}
K	adiabatic compressibility	4.484E-10	kg m^{-1} s^{-2}	calculated	κ'	7.2E-10	kg m^{-1} s^{-2}
δ_t	thermal diffusion length	2.13E-07	m	calculated			
k_t	thermal wave vector	4.68E+06	m^{-1}	calculated			

Table 1 Data used in the spreadsheet calculation of Figure 7 [72], See also http://webbook.nist.gov/cgi/cbook.cgi?ID=C544763&Mask=4

Note that the latent heat of fusion of the droplet is 3.4×10^{-20} J which is much less than the heat accumulation over 300 cycles from Figure 7. At 1 MHz 300 cycles takes 300 μs. Of course, the heat accumulation will not go on increasing indefinitely. Either it is transferred into melting and suppression of further nucleus growth or as the temperature rises steady state, non-oscillatory thermalisation mechanisms will redistribute the heat.

At 1 MHz, the thermal diffusion length in water is around 200 nm, a large distance in comparison to the size of a critical nucleus (Figure 5). Finally, the entire effect can be reversed depending on the adiabatic compressibility of the suspending phase (In water below 4 °C the adiabatic compressibility is negative) and on the relative magnitudes of Γ and Γ'.

4.3. Approximate analytic expression for rectified heating of a droplet in a suspending medium

Finally, an analytic expression can be obtained for the heating effect Q (Joules) over a large number of cycles ($n \to \infty$) which involves integrating Equation 10.

Equation 11

$$Q = \int q.dt$$

To do this the following identity is used

Equation 12

$$\lim_{T\to\infty} \frac{1}{2T} \int_{-T}^{T} e^{i\alpha sin\omega t}.dt = \ J_0(\alpha)$$

Here

$$\propto = {}^{\kappa \Delta p_0}/_{i}$$

We set

$$T = {}^{3\pi n}/_{\omega}$$

So that the integration is carried out over the number of cycles of the pressure wave to which the droplet is subjected.

combining Equation 9 through Equation 12 gives

Equation 13

$$\mathbf{Q} = \lim_{n\to\infty} \frac{3\mathbf{n}}{\omega}\left(\frac{3V_p}{2\pi} J_0\left(\kappa p_0/_i\right)\right)^{2/3} p_o \tau \left[\left(\kappa - \frac{1}{\rho c^2}\right)\Big/_{\beta} - \left(\kappa' - \frac{1}{\rho' c'^2}\right)\Big/_{\beta'}\right]\Big/ \delta_t$$

The same caveat must be applied to this equation as to the results of the numerical calculation presented in Figure 7; that is that slower dissipatory processes neglected will take over as the temperature difference between the drop and its surroundings increases and the effect of thermal pumping will diminish over time until it reaches a steady state. In the work cited above [71], the waxing out temperature in the eicosane fell by 9.5 °C but was not completely suppressed.

4.4. Contribution of the intrinsic material ultrasound attenuation

The above calculation does not take into account the differential thermal dissipation between the suspending and dispersed phases arising from their differing intrinsic acoustic attenuation which contributes in addition to the rectified thermal scattering.

This can be written as the difference between the energy dissipation between the pure suspending phase and the dissipation when a single embryo is placed into the ultrasound field.

Ignoring the time dependence, we can write the ultrasound field intensity as a function of distance as

$$I = I_0 \exp(-\propto_s z)$$

Where I_0 is the acoustic intensity, $\propto_s$ is the attenuation in the suspending phase (Np m^{-1}) and z is the distance over which the attenuation takes place which in this instance is twice the particle radius (See Table 1 for data). We can write down a similar relation for the particle, given that the attenuation in the particulate medium is $\propto_p$ Np m^{-1}.

$$I' = I_0 \exp(-\propto_p z)$$

Over the length of the particle and across the diameter of the particle the dissipation is then

Equation 14

$$I - I' = I_0\, 4\pi r_p^2 \left(exp[-\alpha_s\, 2r_p]) - exp[-\alpha_p 2r_p]\right)$$

Using the data in Table 1 $I - I'$ has the value of 1.22E-24 W which when integrated over 300 cycles as in Figure 7 is an insignificant 3.7E-28 J. It would require 10^{12} s for the energy transfer through differential heating via intrinsic attenuation to equal that of the rectified thermal diffusion process. Even for the case outlined in the next section where the attenuation coefficient has risen 400 fold it would require over 10^9 s to equal the rectified thermal diffusion process.

4.5. The effect of phase change on ultrasound propagation

This treatment thus far ignores the impact of phase change. In terms of interaction with an oscillating pressure wave, there is a big difference between the interaction with an undercooled crystallising system and one at its melting point. (Figure 8).

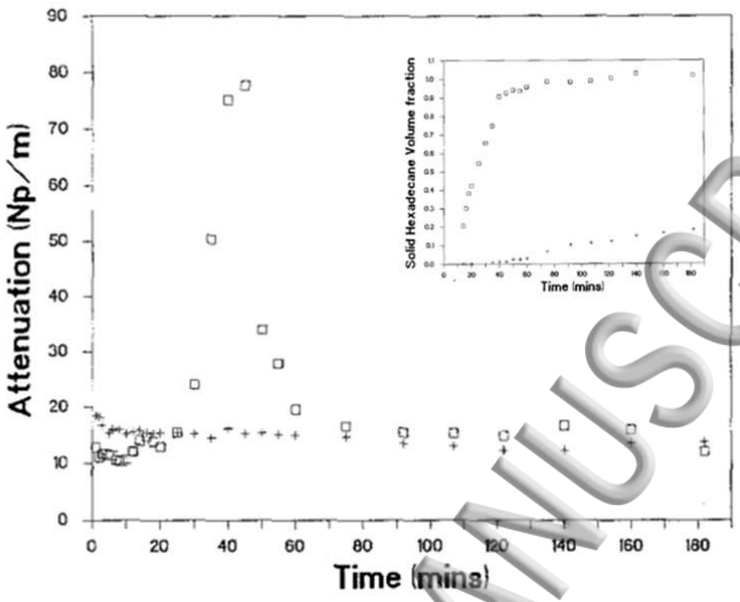

Figure 8 Variation of attenuation coefficient with time at 3 °C for n-hexadecane-in-water emulsions with different mean droplet diameters (d_{32} = 3.3 µm for (□) and 0.36 µm for (+). Inset is the solid content temporal evolution indicating that for the coarser emulsion which shows the attenuation peak, crystallisation is almost complete whilst in the finer emulsion crystal growth has only just begun. [73]

Phase change introduces an additional rectified heating effect which is referred to in [30] a theoretical investigation of crystallization nuclei undergoing radially symmetric oscillations in supercooled liquids and supersaturated solutions exposed to a sound field. According to these authors, periodic crystallization and melting processes occurring in the course of pressure oscillations are shown to result in higher amplitudes. This enhances the nonlinear interaction of sound with an oscillating nucleus which results in the phenomenon of rectified heat transfer, i.e. a slow (as against the sound cycle) process of heat pumping into a nucleus. They show that phase transformations may markedly increase the absorption and dispersion of the speed of sound propagating in crystallizing liquids as compared with liquids containing solid particles without phase transformations.

Finally, [74] points out the similarity between the form of the nucleus Gibbs Free energy function and the quantum tunnelling potential. The advantage of this approach is that all possible paths between the liquid suspending fluid and the embryo can be explored and provides a bridge

between the two state (or many state) models and CNT. In particular, molecular attachment theories permit the one or two at a time attachment of molecules from the liquid state to the growing embryo or nucleus. Yet, for most of the existence of the embryo, each step remains energetically unfavourable so the question is how can 400 molecules (Figure 5) suddenly find themselves in a stable nucleus? Quantum tunnelling provides an approach to this problem which does not restrict itself to one or two steps but permits a proliferation of more or less unlikely steps, the overall probability of transition being the sum over all possible paths. This suggests that a molecular modelling approach which permits the enumeration of all possible paths to a stable nucleus may be a profitable next step towards the solution of the nucleation problem.

5. Conclusion

Our data shows that the Classical Nucleation Theory remains a sound basis from which to understand nucleation in food colloids and in analogous model systems such as those of n-alkanes. The theory has been examined using a number of techniques but most usefully with ultrasound velocity spectrometry. Ultrasound velocity spectrometry measurements have many advantages for the study of nucleating systems compared to light scattering and NMR due to its sensitivity at low solid contents and its ability to measure true solid contents in the nucleation and early crystal growth stages. Unlike other techniques ultrasound attenuation spectroscopy also responds to critical fluctuations in the induction region and to melting and crystallisation phenomena close to the melting point. A potential prize is unprecedented control over the nucleation step with obvious implications for all industries in which crystal growth is important.

In addition to its use as an analytical tool we show, that a periodic pressure fluctuation such as a quasi-continuous (as opposed to a pulse comprising only a few pressure cycles) ultrasound field can alter the nucleation process, even at very low acoustic intensity.

In previous work, it has been assumed that low power ultrasound is not material altering [37]. The current work challenges that assumption meaning that care must be taken when using ultrasound techniques to ensure that the measurements do not alter the studied processes. This can be done for example by repeating experiments at different power levels, measurement results in PE experiments should be independent of power. If they are not, then the measurement technique is changing the material. This treatment of rectified heat flow does not apply to PE measurements where short pulses are concerned, nevertheless care should be taken over this point. With regard to micro-emulsions such as Ouzo, CNT will not apply to micro-emulsions in the way it is applied in this

paper because of the small surface energy term. Nevertheless, it is possible that the region over which micro-emulsions are stable may be widened (or reduced) through the application of low power quasi-static ultrasound since they destabilise once the surface energy term increases relative to the volume term.

Low power quasi-continuous ultrasound is a potentially powerful tool for the control of nucleation; quasi-continuous ultrasound fields may enhance or suppress nucleation and the criteria to determine such effects have been derived in this paper.

There is considerably more work to be done on the interaction between low intensity oscillating pressure fields (<10KPa) and nucleating colloidal systems. However, the conclusions of this paper are relevant to the understanding of nucleation behaviour and to the practical application of colloidal systems in foods, pharmaceuticals, agro-chemicals, cosmetics and personal products.

Acknowledgements

The author has benefitted from discussions with Mel Holmes, Rammile Ettelaie and Martin Pick in the School of Food Science and Nutrition. The treatment of rectified thermal diffusion and nucleation has been greatly influenced by discussions with Ken Lewtas (Lewtas Sci-Tec) and Peter Bawden (Bawden and Associates). Support for parts of this work from the EPSRC in the form of grant EP/M026310/1 is acknowledged.

Bibliography

1 C. Méndez-Velasco and H.D. Goff, Int. Dairy J. 21, 540 (2011).

2 K.E. Allen, B.S. Murray, and E. Dickinson, Food Hydrocoll. 22, 690 (2008).

3 E. Dickinson, Curr. Opin. Colloid Interface Sci. 15, 40 (2010).

4 G. Davidov-Pardo, I., Joye, D. J. McClements, in Adv. Protein Chem. Struct. Biol. Acad. Press, edited by D. Rossen (Academic Press, 2015).

5 M.J.W. Povey, Food Hydrocoll. 42, 118 (2014).

6 S. A. Hindle, M.J.W. Povey, and K.W. Smith, J. Am. Oil Chem. Soc. 79, 993 (2002).

7 N. Kaneko, T. Horie, S. Ueno, J. Yano, T. Katsuragi, and K. Sato, J. Cryst. Growth 197, 263 (1999).

8 S. Ueno, Y. Hamada, and K. Sato, Cryst. Growth Des. 3, 935 (2003).

9 K. Sato, L. Bayés-García, T. Calvet, M.À. Cuevas-Diarte, and S. Ueno, Eur. J. Lipid Sci. Technol. 115, 1224 (2013).

10 T. Katsuragi, N. Kaneko, and K. Sato, Colloids and Surfaces B-Biointerfaces 20, 229 (2001).

11 K. Sato and S. Ueno, Curr. Opin. Colloid Interface Sci. 16, 384 (2011).

12 K. Sato, Chem. Eng. Sci. 56, 2255 (2001).

13 I. Burgaud, E. Dickinson, and P. V. Nelson, Int. J. Food Sci. Technol. 25, 39 (2007).

14 S. Schultz, G. Wagner, K. Urban, and J. Ulrich, Chem. Eng. Technol. 27, 361 (2004).

15 A. Håkansson, Dynamic Modelling of Emulsification in High Pressure Homogenizers (n.d.).

16 A. Forgiarini, J. Esquena, C. Gonzalez, and C. Solans, Langmuir 17, 2076 (2001).

17 B. Abismail, J.P. Canselier, A.M. Wilhelm, H. Delmas, C. Gourdon, H. Delams, and C. Gourdon, Ultrason. Sonochem. 6, 75 (1999).

18 F. Chemat, Zill-E-Huma, and M.K. Khan, Ultrason. Sonochem. 18, 813 (2011).

19 S.A. Vitale and J.L. Katz, Langmuir 19, 4105 (2003).

20 M.D.L. de Castro and F. Priego-Capote, Ultrason. Sonochem. 14, 717 (2007).

21 H. Li, H.R. Li, Z.C. Guo, and Y. Liu, Ultrason. Sonochem. 13, 359 (2006).

22 M. Jiang, C.D. Papageorgiou, J. Waetzig, A. Hardy, M. Langston, and R.D. Braatz, Cryst. Growth Des. 15, 2486 (2015).

23 M.H. Zamanipoor and R.L. Mancera, TRENDS FOOD Sci. Technol. 50, 264 (2016).

24 Z. Zhang, D.-W. Sun, Z. Zhu, and L. Cheng, Compr. Rev. Food Sci. FOOD Saf. 14, 303 (2015).

25 J.A. Rincon-Cardona, L.M. Agudelo-Laverde, M.L. Herrera, and S. Martini, J. Am. OIL Chem. Soc. 92, 473 (2015).

26 T.G. Leighton, The Acoustic Bubble, Academic Press, London (1994).

27 R.C. Chow, D. Atkins, S. Singleton, R. Mettin, B. Lindinger, T. Kurz, W. Lauterborn, M. Povey, and R. Chivers, Water Prop. Food, Pharm. Biol. Mater. 9, 613 (2006).

28 R. Chow, R. Blindt, R. Chivers, and M. Povey, Ultrasonics 43, 227 (2005).

29 R. Chow, R. Blindt, R. Chivers, and M. Povey, Ultrasonics 41, 595 (2003).

30 V.A. Akulichev and V.A. Bulanov, J. Heat Mass Transf. 26, 289 (1983).

31 M.J.W. Povey and R.E. Challis, Adv. Dairy Chem. 2, 709 (2006).

32 S. Hindle, M.J.W. Povey, and K. Smith, J. Colloid Interface Sci. 232, 370 (2000).

33 M.J.W. Povey, S.A. Hindle, A. Aarflot, and H. (University of B. Hoiland, Cryst. Growth Des. 6, 297 (2006).

34 M.J.W. Povey, T.S. Awad, R. Huo, and Y.L. Ding, Eur. J. Lipid Sci. Technol. 111, 236 (2009).

35 E. Dickinson, F.J. Kruizenga, M.J.W. Povey, and M. van der Molen, Colloids Surfaces A Physicochem. Eng. Asp. 81, 273 (1993).

36 F.G. Bijnen, H. van Aalst, P.-Y. Baillif, J.C. Blonk, D. Kersten, F. Kleinherenbrink, R. Lenke, and M.L. vander Stappen, Powder Technol. 124, 188 (2002).

37 M.J.W. Povey, Ultrasonic Techniques for Fluids Characterization (Academic Press, San Diego, Calif. ; London, 1997).

38 D.L. Ericson, X. Yin, A. Scalia, Y.N. Samara, R. Stearns, H. Vlahos, R. Ellson, R.M. Sweet, and A.S. Soares, JALA 21, 107 (2016).

39 A. Rigolle, I. Foubert, J. Hettler, E. Verboven, A. Martens, R. Demuynck, and K. den Abeele, Innov. FOOD Sci. Emerg. Technol. 33, 289 (2016).

40 A. Rigolle, I. Foubert, J. Hettler, E. Verboven, R. Demuynck, and K. den Abeele, FOOD Res. Int. 75, 115 (2015).

41 S.T. Beckett, The Science of Chocolate (RSC publishing, 2002).

42 J.C. Fisher, J.H. Hollomon, and D. Turnbull, J. Appl. Phys. 19, 775 (1948).

43 D. Turnbull and R.L. Cormia, J. Chem. Phys. 34, 820 (1961).

44 D. Turnbull and C.R. L., Acta Metall. 8, 747 (1960).

45 D. Turnbull, J. Appl. Phys. 21, 1022 (1950).

46 R.J. Davey, S.L.M. Schroeder, and J.H. Ter Horst, Angew. Chemie - Int. Ed. 52, 2167 (2013).

47 S. Auer and D. Frenkel, Annu. Rev. Biophys. Biophys. Chem. 55, 333 (2004).

48 P.G. Vekilov, Cryst. Growth Des. 10, 5007 (2010).

49 S. Prestipino, A. Laio, and E. Tosatti, Phys. Rev. Lett. 108, 225701 (2012).

50 T.L. Threlfall and S.J. Coles, CrystEngComm. 18, 369 (2016).

51 M.R. Singh and D. Ramkrishna, Chem. Eng. Sci. 107, 102 (2014).

52 D. V Alexandrov and A.P. Malygin, Model. Simul. Mater. Sci. Eng. 22, (2014).

53 P.R. tenWolde and D. Frenkel, Science (80-.). 277, 1975 (1997).

54 P.J. Desre, Philos. Mag. Lett. 69, 261 (1994).

55 F. Sheng, X. Lai, M. Holmes, and M.J.W. Povey, In Situ Monitoring of Crystal Volume Fraction during the Batch Crystallization of Copper Sulphate Pentahydrate from Aqueous Solution Depending on Ultrasonic Velocity Measurement Fei Sheng, Xiaojun Lai, Melvin Holmes and Malcolm J. W. Povey (2016) In preparation.

56 E. Simone, A.N. Saleemi, N. Tonnon, and Z.K. Nagy, Cryst. Growth Des. 14, 1839 (2014).

57 E. Simone, A.N. Saleemi, and Z.K. Nagy, Chem. Eng. Res. Des. 92, 594 (2014).

58 E. Simone, A.N. Saleemi, and Z.K. Nagy, Chem. Eng. Technol. 37, 1305 (2014).

59 E. Simone, A.N. Saleemi, and Z.K. Nagy, Org. Process Res. Dev. 19, 167 (2015).

60 E. Simone and Z.K. Nagy, CRYSTENGCOMM 17, 6538 (2015).

61 E. Simone, W. Zhang, and Z.K. Nagy, Cryst. Growth Des. 15, 2908 (2015).

62 E. Simone, W. Zhang, and Z.K. Nagy, J. Chem. Technol. Biotechnol. 91, 1461 (2016).

63 S.L. Petersson B, Anjou K, Fette. Seifen. Anstrichm. 6, 225 (1985).

64 J.E. Norton, P.J. Fryer, J. Parkinson, and P.W. Cox, J. Food Eng. 95, 172 (2009).

65 S. Ozilgen, C. Simoneau, J.B. German, M.J. Mccarthy, and D.S. Reid, J. Sci. Food Agric. 61, 101 (1993).

66 S.M. Hodge and D. Rousseau, J. Am. Oil Chem. Soc. 82, 159 (2005).

67 E. Anoardo, G. Galli, and G. Ferrante, Appl. Magn. Reson. 20, 365 (2001).

68 P.S. Belton and Y. Wang, in Magn. Reson. Food Sci. A View To Futur., edited by Webb, GA and Belton, PS and Gil, AM and Delgadillo, I (2001), pp. 145–156.

69 S. Auer and D. Frenkel, Nature 413, 711 (2001).

70 P.D. Edmonds, in Methods Exp. Phys. Vol. 19 (1981).

71 M.J.W. Povey and K. Lewtas, Patent GB1603981.0 (2016).

72 J.R. Allegra and S.A. Hawley, J. Acoust. Soc. Am. 51, 1545 (1972).

73 E. Dickinson, D.J. McClements, and M.J.W. Povey, J. Colloid Interface Sci. 142, 103 (1991).

74 J.C. Martinez, J. Colloid Interface Sci. 205, 476 (1998).

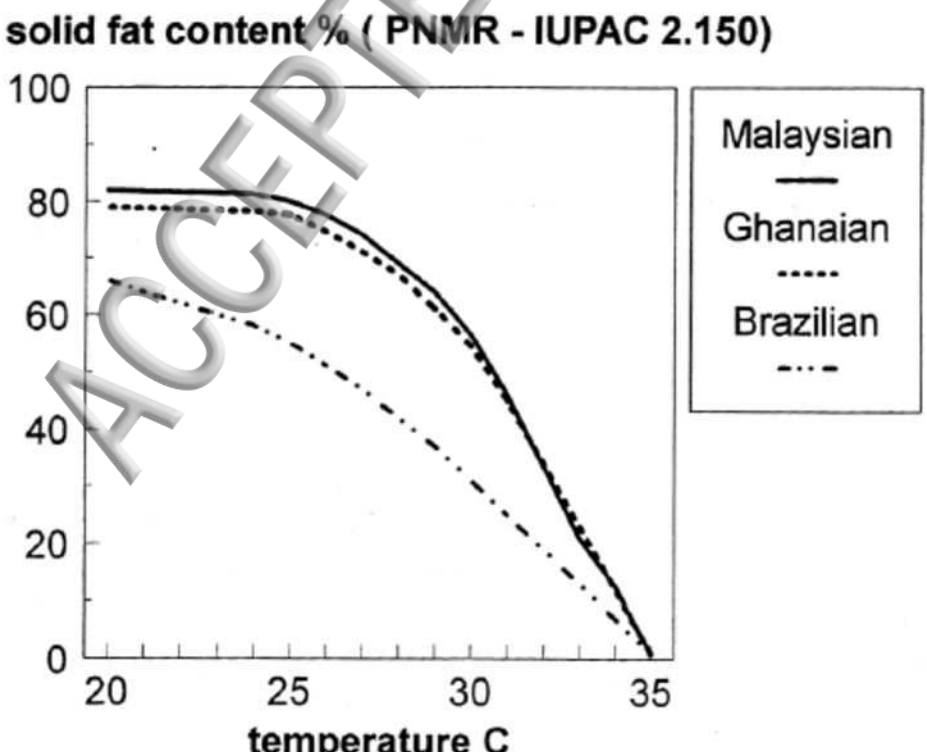
solid fat content % (PNMR - IUPAC 2.150)
100
80
60
40
20
0
20
25
30
35
temperature C
Malaysian
Ghanaian
Brazilian

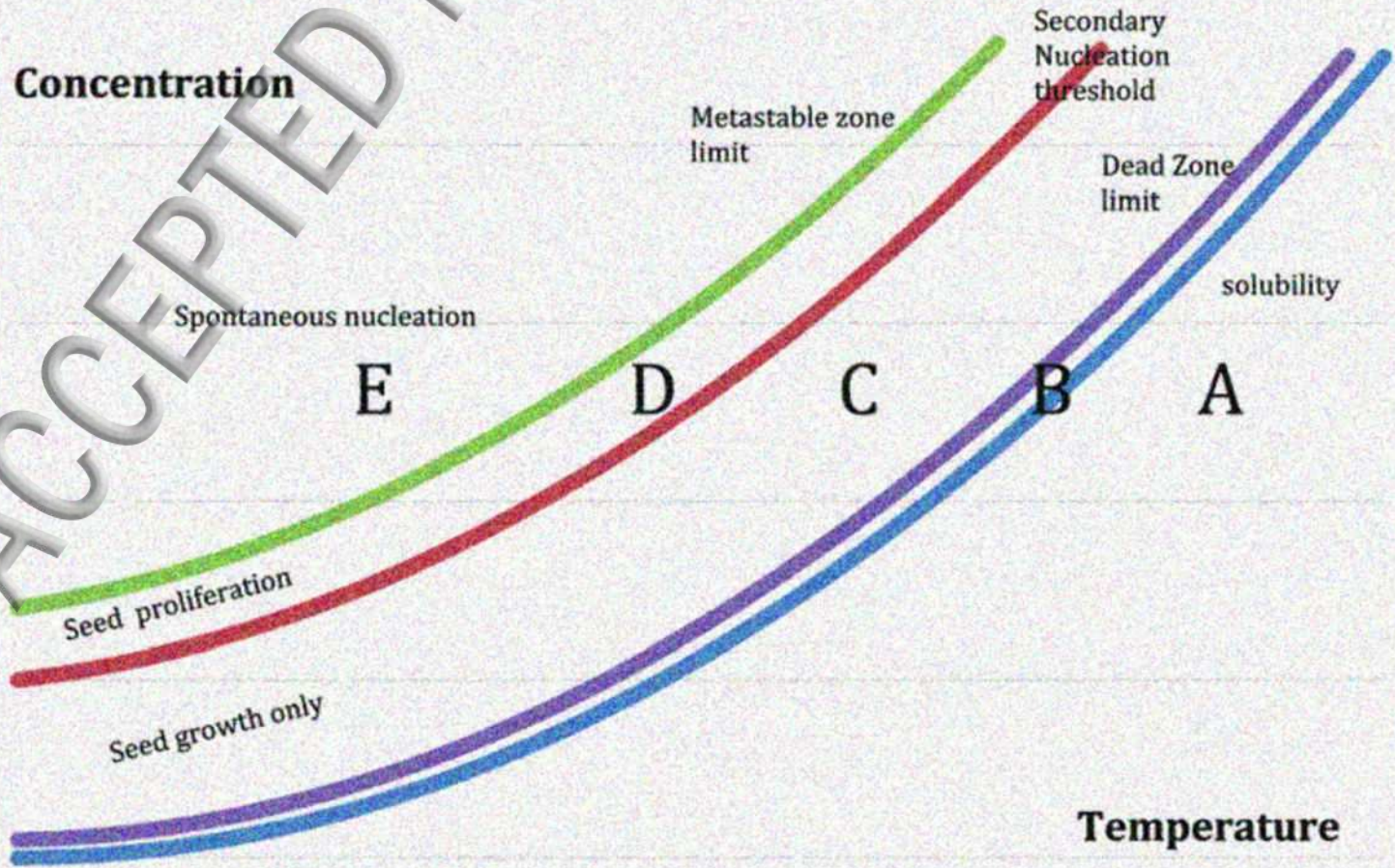
Concentration
Secondary
Nucleation
threshold
Metastable zone
limit
Dead Zone
limit
solubility
Spontaneous nucleation
E
D
C
B
A
Seed proliferation
Seed growth only
Temperature

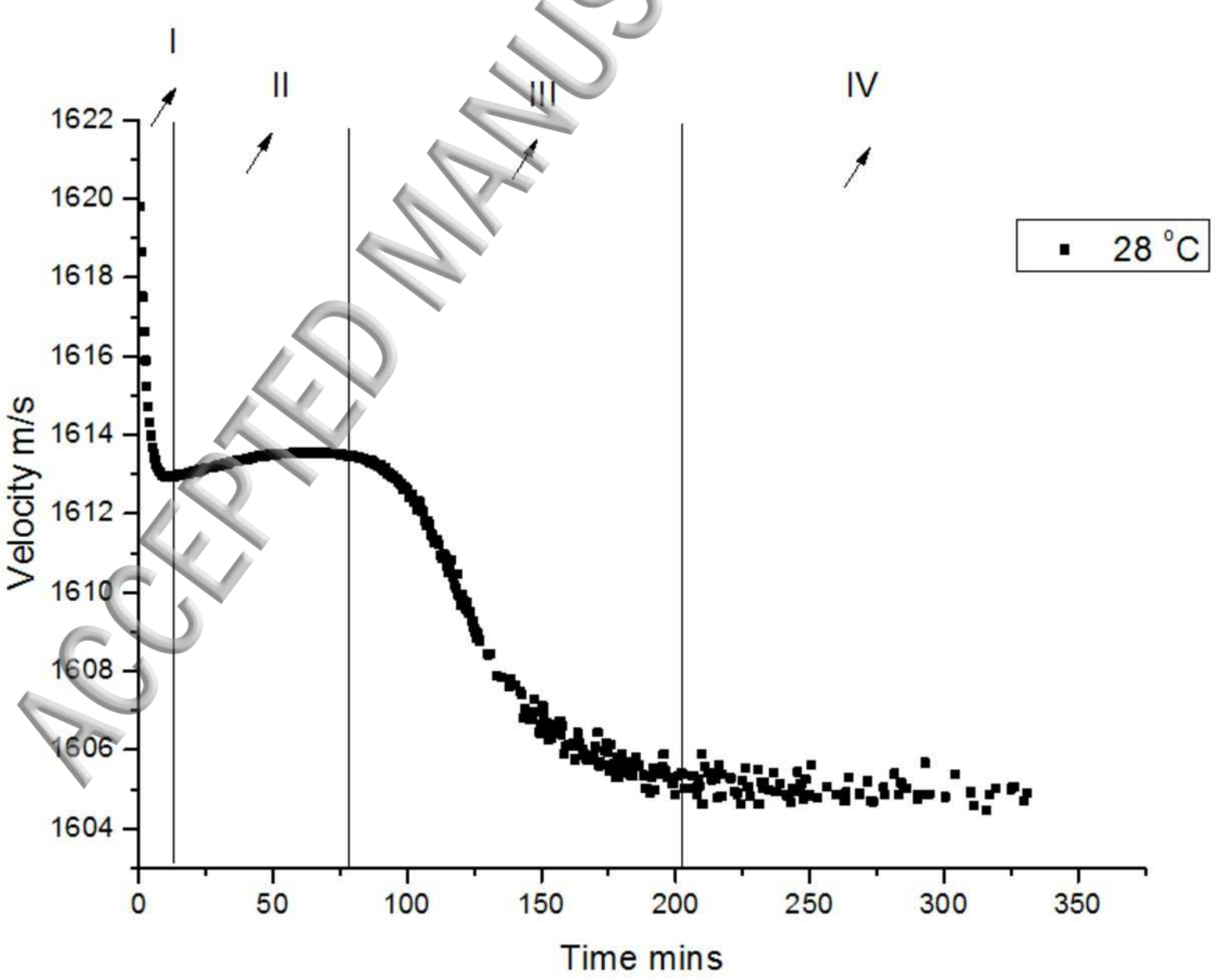

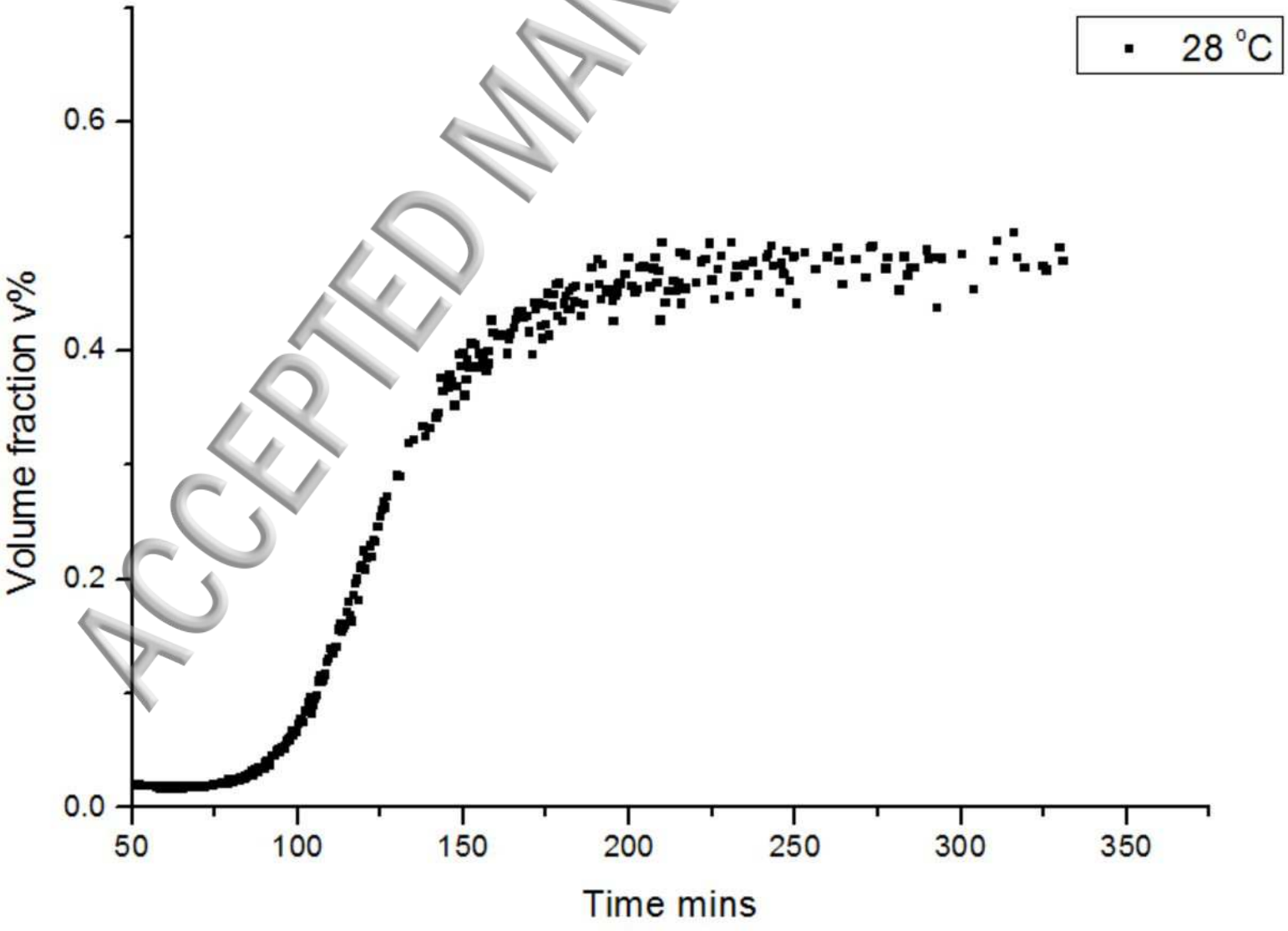

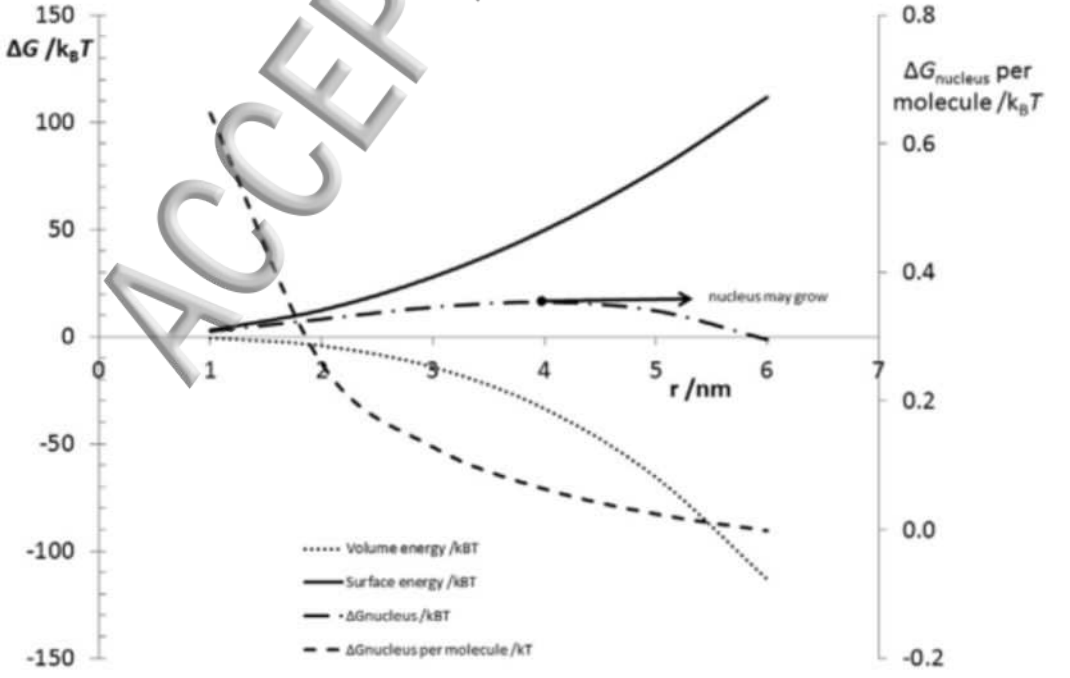
ΔG /k_BT
ΔG_nucleus per molecule /k_BT
r /nm
nucleus may grow
Volume energy /kBT
Surface energy /kBT
ΔGnucleus /kBT
ΔGnucleus per molecule /kT

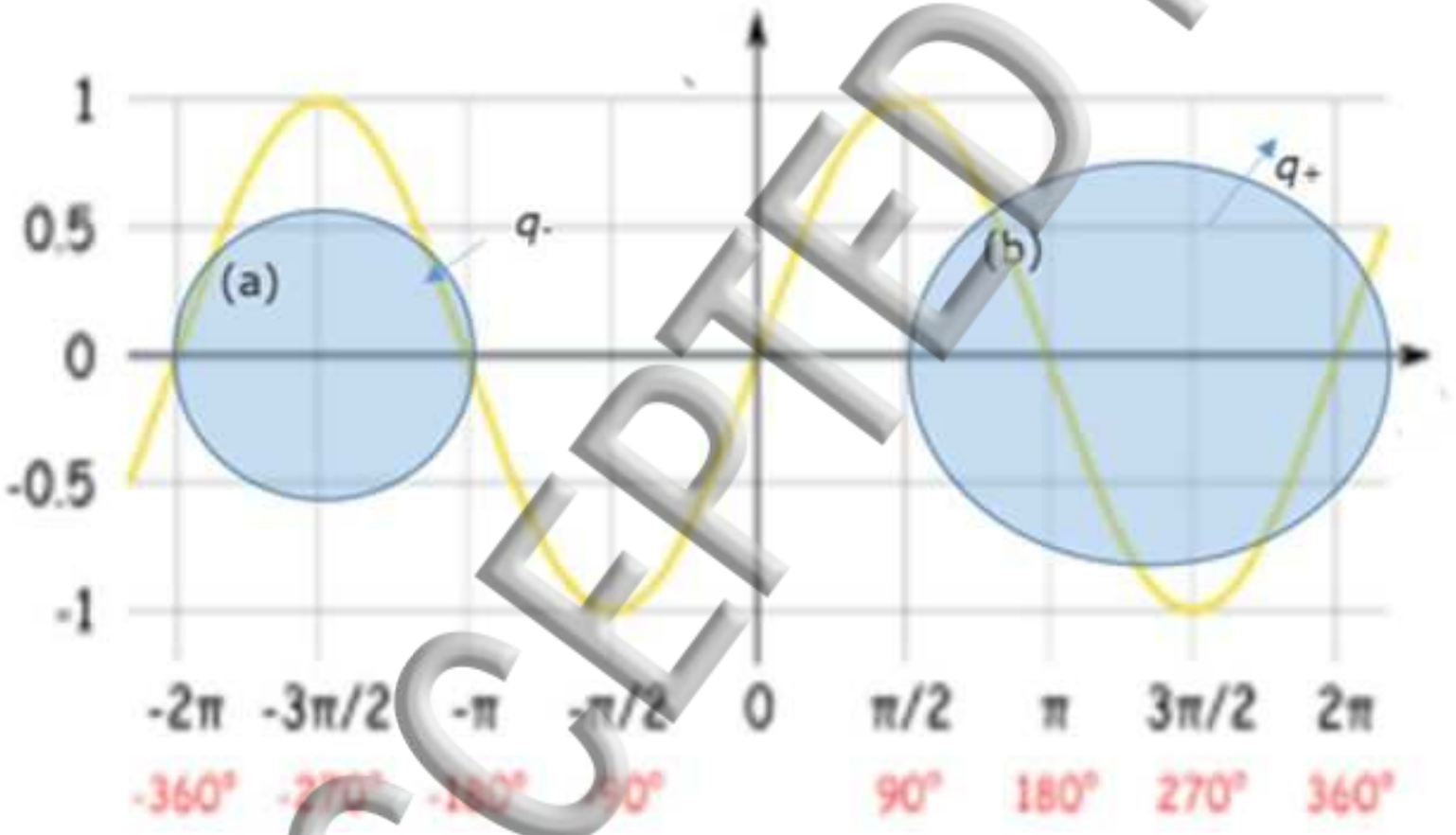

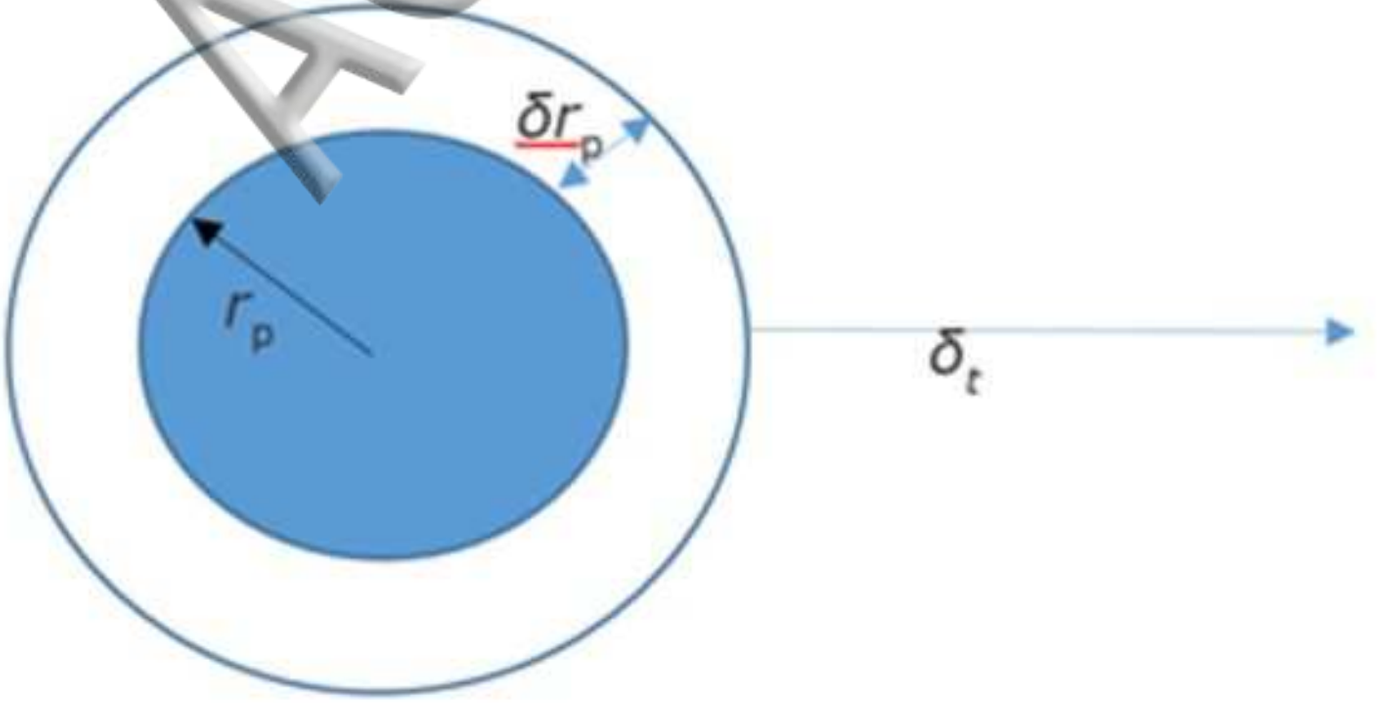

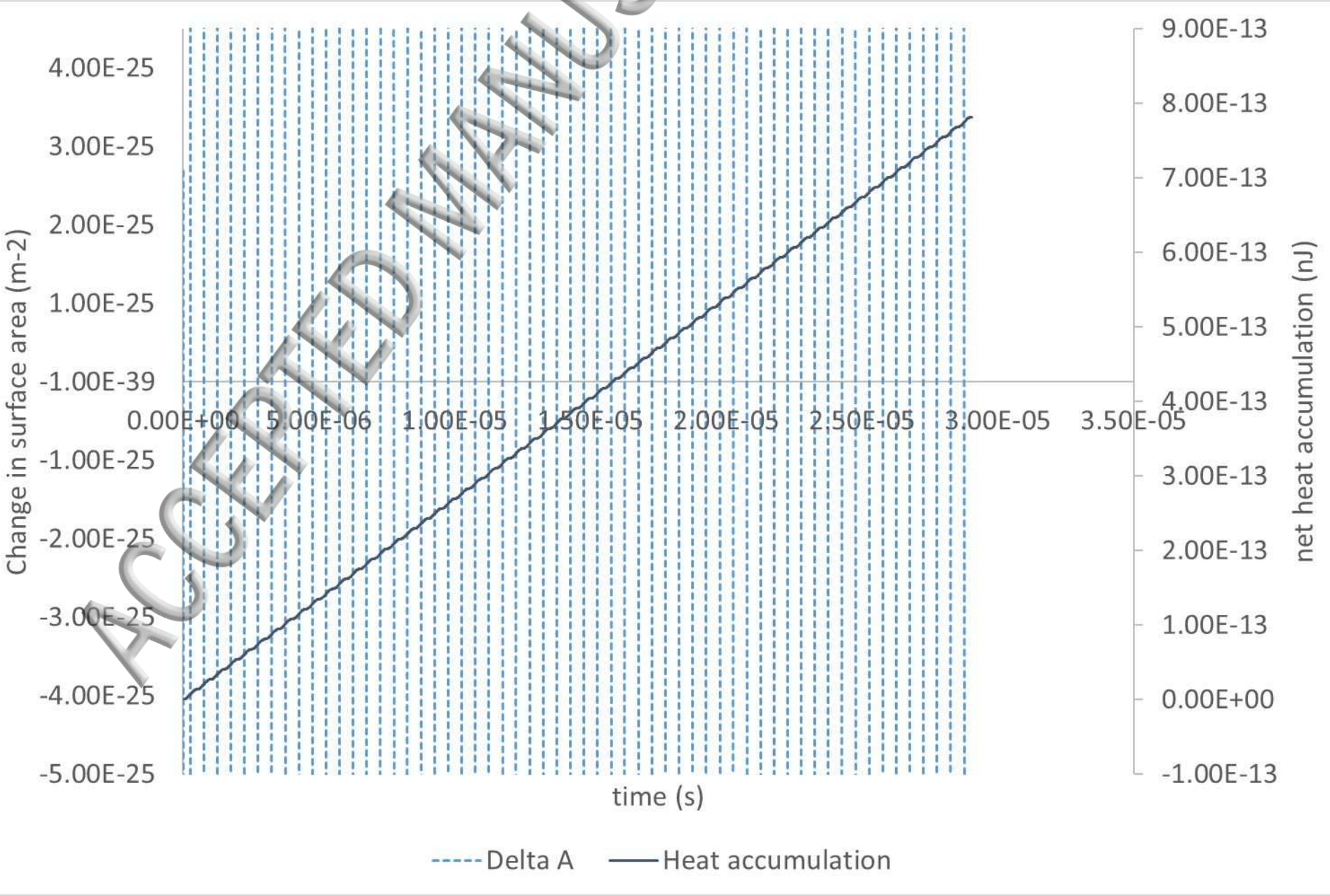

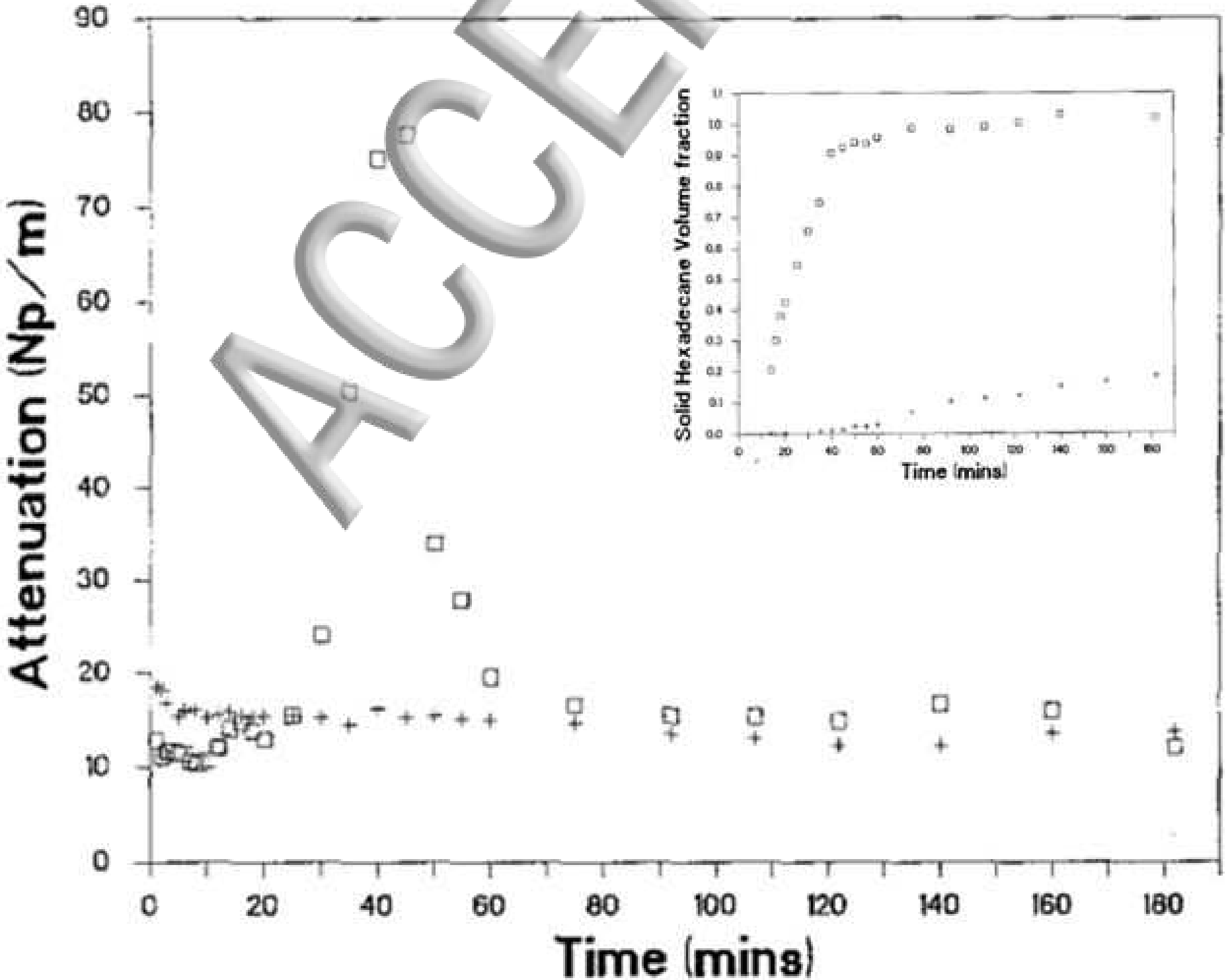
Attenuation (Np/m)
90
80
70
60
50
40
30
20
10
0
0
20
40
60
80
100
120
140
160
180
Time (mins)
Solid Hexadecane Volume fraction
Time (mins)